Jamming Strategies in Wireless Source Localization Systems

Musa Furkan Keskin, Cuneyd Ozturk, Suat Bayram, and Sinan Gezici

***Abstract*—We consider optimal jamming strategies in wireless source localization systems, where anchor nodes estimate positions of target nodes in the presence of jammers that emit zero-mean Gaussian noise. The Cramér-Rao lower bound (CRLB) for target location estimation is derived and the problem of optimal power allocation for jammer nodes is formulated to maximize the average CRLB for target nodes under total and peak power constraints. Exploiting the special problem structure and successive convex approximation techniques, we develop an iterative algorithm that transforms the original non-convex problem into a sequence of convex geometric programs. In addition, we present a closed-form solution that is asymptotically optimal. Numerical results demonstrate the improved jamming performance of the proposed solutions over the uniform power allocation strategy.**

***Index Terms*– Jamming, wireless localization, power allocation, geometric programming, successive convex approximation.**

I. Introduction

In wireless localization systems, location estimation is commonly performed via signal exchanges between *anchor nodes* with known positions and *target nodes* whose positions are to be estimated [1], [2]. Depending on the signaling procedure, localization systems can be classified into two groups; namely, *self localization* systems and *source localization* (or, network-centric localization) systems [1]. In the self localization approach, target nodes estimate their own locations using signals transmitted by anchor nodes while in the source localization case, the anchor network performs position estimation of target nodes based on signals emitted by these nodes.

To degrade performance of wireless localization systems (i.e., to reduce localization accuracy of target nodes), *jammer nodes* can transmit jamming signals that disturb the localization signals between anchor and target nodes [3]. Investigation of jamming strategies is crucial for location-aware networks to determine adversarial capabilities of jammer nodes and also to develop effective countermeasures against jamming. In the literature, jamming strategies in wireless localization networks have been investigated within the context of self localization systems [3], [4], and in particular GPS systems [5], [6]. In [5], a performance analysis for GPS jamming and anti-jamming techniques is presented. Similarly, the work in [6] proposes an anti-jamming GPS receiver that reduces the impact of carrier phase errors. In [3], jamming of wireless networks relying on self localization is investigated and optimal power allocation solutions for jammer nodes are characterized by adopting the Cramér-Rao lower bound (CRLB) on the localization error of target nodes as the performance metric. The work in [4] designs a more generic framework for jammer power allocation by using the restricted Bayesian approach. Although the problem of optimal power allocation for jammer nodes has been addressed for self localization systems in the literature, there exist no studies that consider jamming strategies for wireless source localization systems. Due to a different signal exchange mechanism compared to self localization, the source localization configuration yields a challenging non-convex optimization problem (as opposed to linear programs in [3], [4]) which necessitates the design of new jamming approaches.

In this letter, we investigate a generic localization scenario in which jammer nodes are employed to degrade the performance of a wireless source localization system. We derive the CRLB for target localization in the presence of zero-mean Gaussian jamming signals and formulate the problem of optimal power allocation among jammer nodes to maximize the average CRLB for target nodes under total and peak power constraints. Then, we propose a geometric programming (GP) based iterative algorithm by employing successive convex approximation (SCA) tools. In addition, we provide an asymptotically optimal closed-form solution. Numerical results illustrate the performance gains of the proposed techniques.

M. F. Keskin is with the Department of Electrical Engineering, Chalmers University of Technology, 41296, Gothenburg, Sweden (e-mail: furkan@chalmers.se). C. Ozturk and S. Gezici are with the Department of Electrical and Electronics Engineering, Bilkent University, 06800, Ankara, Turkey (e-mails: {cuneyd,gezici}@ee.bilkent.edu.tr). S. Bayram is with Suat Bayram Muhendislik Hizmetleri, 06760, Ankara, Turkey (e-mail: suat.bayram@paneratech.com)

II. System Model and Problem Formulation

Consider a two-dimensional wireless source localization system with N_A anchor nodes located at $\boldsymbol{y}_j \in \mathbb{R}^2$ for $j = 1, \ldots, N_A$. Target nodes are randomly located in the environment in such a way that a target node exists at location $\boldsymbol{x}_i \in \mathbb{R}^2$ with probability w_i for $i = 1, \ldots, N_T$, where N_T is the number of possible target positions, $\sum_{i=1}^{N_T} w_i = 1$ and $w_i \geq 0 \ \forall i$. In addition, there exist N_J jammer nodes located at $\boldsymbol{z}_\ell \in \mathbb{R}^2$ for $\ell = 1, \ldots, N_J$. In the source localization scenario, the position of a target node is estimated by the network of anchor nodes based on received signals emitted by that target node. It is assumed that some form of multiplexing is employed so that channels between a target node and anchor nodes are all orthogonal.While the anchor nodes aim to perform accurate estimation of target positions, the objective of jammer nodes is to degrade the localization performance by transmitting zero-mean Gaussian noise [7].

Let $\mathcal{A}_i$ denote the set of anchor nodes that are connected to the target node at the ith position (i.e., location $\boldsymbol{x}_i$), which can be partitioned as $\mathcal{A}_i \triangleq \mathcal{A}_i^L \cup \mathcal{A}_i^{NL}$ where $\mathcal{A}_i^L$ and $\mathcal{A}_i^{NL}$ represent the sets of anchors nodes with line-of-sight (LOS) and non-line-of-sight (NLOS) connections to that target node, respectively. In addition, the set of jammer nodes is represented by $\mathcal{J} = \{1, \ldots, N_J\}$. Then, the received signal at anchor node j coming from the target node at position i can be expressed as [3], [8]

$$r_{ij}(t) = \sum_{k=1}^{L_{ij}} \alpha_{ij}^k s_{ij}(t-\tau_{ij}^k) + \sum_{\ell \in \mathcal{J}} \gamma_{\ell j} \sqrt{P_\ell^J} v_{\ell i j}(t) + n_{ij}(t) \quad (1)$$

for $t \in [0, T_{\rm obs}]$, $i \in \{1, \ldots, N_T\}$, and $j \in \mathcal{A}_i$, where $T_{\rm obs}$ specifies the observation time, $s_{ij}(t)$ is the transmit signal of the target node at position i intended for anchor node j, α_{ij}^k and τ_{ij}^k denote, respectively, the amplitude and delay of the kth multipath component between the target node at position i and anchor node j, L_{ij} is the number of paths between the target node at position i and anchor node j, $\gamma_{\ell j}$ represents the channel coefficient between anchor node j and jammer node ℓ, and P_ℓ^J is the transmit power of jammer node ℓ. In addition, $\sqrt{P_\ell^J} v_{\ell i j}(t)$ and $n_{ij}(t)$ denote, respectively, the jammer noise and the measurement noise, both of which are assumed to be independent zero-mean white Gaussian random processes, where the average power of $v_{\ell ij}(t)$ is equal to one and that of $n_{ij}(t)$ is $N_0/2$ [3]. It is modeled that $n_{ij}(t)$ is independent for all i, j, and $v_{\ell ij}(t)$ is independent for all i, j, ℓ due to the assumption of orthogonal channels. Furthermore, τ_{ij}^k in (1) represents the delay term, which is given by $\tau_{ij}^k \triangleq (\|\boldsymbol{y}_j - \boldsymbol{x}_i\| + b_{ij}^k)/c$, where $b_{ij}^k \geq 0$ and c denote, respectively, the range bias of the kth path and the speed of propagation.

Via similar steps to those in [3], [8], the equivalent Fisher information matrix $\boldsymbol{J}_i(\boldsymbol{p}^J)$ corresponding to the target node at position i is obtained as

$$\boldsymbol{J}_i(\boldsymbol{p}^J) = \sum_{j \in \mathcal{A}_i^L} \frac{\lambda_{ij}}{N_0/2 + \boldsymbol{a}_j^T \boldsymbol{p}^J} \boldsymbol{\phi}_{ij} \boldsymbol{\phi}_{ij}^T \tag{2}$$

$$\lambda_{ij} \triangleq 4\pi^2 E_{ij} \beta_{ij}^2 |\alpha_{ij}^1|^2 (1 - \xi_{ij})/c^2 \,, \tag{3}$$

$$\boldsymbol{a}_j \triangleq \left[|\gamma_{1j}|^2 \cdots |\gamma_{N_J j}|^2 \right]^T , \tag{4}$$

$$\boldsymbol{p}^J \triangleq \left[P_1^J \cdots P_{N_J}^J \right]^T , \ \boldsymbol{\phi}_{ij} \triangleq [\cos\varphi_{ij} \ \ \sin\varphi_{ij}]^T \tag{5}$$

where E_{ij} and β_{ij} are, respectively, the energy and the effective bandwidth of $s_{ij}(t)$, ξ_{ij} is the path-overlap coefficient satisfying $0 \leq \xi_{ij} \leq 1$ [8][1], φ_{ij} represents the angle between the target node at position i and anchor node j, and $\boldsymbol{a}_j$ denotes the vector of channel gains between the jammer nodes and anchor node j. The CRLB constitutes a lower bound on the mean-squared error (MSE) of any unbiased estimator $\hat{\boldsymbol{x}}_i$ of target location $\boldsymbol{x}_i$ [9]; that is,

$$\mathbb{E}\left\{ \|\hat{\boldsymbol{x}}_i - \boldsymbol{x}_i\|^2 \right\} \geq \operatorname{tr}\left\{ \boldsymbol{J}_i(\boldsymbol{p}^J)^{-1} \right\} \triangleq C_i(\boldsymbol{p}^J) \tag{6}$$

where $\boldsymbol{J}_i(\boldsymbol{p}^J)$ is given by (2) and $C_i(\boldsymbol{p}^J)$ represents the CRLB for the localization of the target node at position i. From (2)–(5), the CRLB in (6) can be rewritten, after some manipulation, as follows:

$$C_i(\boldsymbol{p}^J) = f_i(\boldsymbol{p}^J)/g_i(\boldsymbol{p}^J) \tag{7}$$

$$f_i(\boldsymbol{p}^J) \triangleq \sum_{j_1 \in \mathcal{A}_i^L} \lambda_{ij_1} \prod_{\substack{j_2 \in \mathcal{A}_i^L \\ j_2 \neq j_1}} \left(\frac{N_0}{2} + \boldsymbol{a}_{j_2}^T \boldsymbol{p}^J \right), \quad g_i(\boldsymbol{p}^J) \triangleq \sum_{j_1 \in \mathcal{A}_i^L} \sum_{\substack{j_2 \in \mathcal{A}_i^L \\ j_2 > j_1}} \lambda_{ij_1} \lambda_{ij_2} \sin^2(\varphi_{ij_1} - \varphi_{ij_2}) \prod_{\substack{j_3 \in \mathcal{A}_i^L \\ j_3 \neq j_1 \\ j_3 \neq j_2}} \left(\frac{N_0}{2} + \boldsymbol{a}_{j_3}^T \boldsymbol{p}^J \right) \tag{8}$$

The purpose of jamming in the proposed source localization scenario is to minimize the localization performance of the wireless system via optimal power allocation among jammer nodes under individual and total power constraints. To that aim, we adopt the CRLB as a measure of localization accuracy since the maximum likelihood (ML) estimator for target location is asymptotically tight to the CRLB in the high SNR regime [9]. Hence, the problem of optimal power allocation for jammer nodes is formulated to maximize the average CRLB for possible target positions under certain constraints as follows:

$$\underset{\boldsymbol{p}^J}{\text{maximize}} \ \sum_{i=1}^{N_T} w_i C_i(\boldsymbol{p}^J) \tag{9a}$$

$$\text{subject to} \ \ \boldsymbol{1}^T \boldsymbol{p}^J \leq P_{\mathrm{T}} \tag{9b}$$

$$0 \leq P_\ell^J \leq P_\ell^{\mathrm{peak}} , \quad \ell = 1, 2, \ldots, N_J \tag{9c}$$

where $C_i(\boldsymbol{p}^J)$ is given by (7), P_{T} is the total power budget for the jammer network, which results from energy consumption restrictions, and P_ℓ^{peak} is the peak power limit for jammer node ℓ, which is imposed by hardware limitations. In (9), we attempt to degrade the average of the best achievable estimation accuracies (i.e., CRLBs) over possible target positions by optimizing jammer powers.

III. Optimal Jammer Power Allocation

In this section, we propose a GP based iterative algorithm to solve the problem (9) by leveraging SCA techniques. In addition, we provide an asymptotically optimal closed-form solution to (9).

A. Jammer Power Allocation via Geometric Programming

Since $g_i(\boldsymbol{p}^J)$ in (8) is positive for any power vector $\boldsymbol{p}^J$ (due to the non-negativity of the terms λ_{ij}, N_0, and $\boldsymbol{a}_j$), the problem in (9) can be rewritten in the epigraph form as [10]

$$\underset{\boldsymbol{p}^J, \boldsymbol{\nu}}{\text{maximize}} \ \ \boldsymbol{w}^T \boldsymbol{\nu} \tag{10a}$$

$$\text{subject to} \ \ \nu_i \, g_i(\boldsymbol{p}^J) \leq f_i(\boldsymbol{p}^J), \ i = 1, \ldots, N_T \tag{10b}$$

$$\text{(9b), (9c)}$$

with $\boldsymbol{w} = [w_1 \ldots w_{N_T}]^T$, where we introduce the slack variables $\boldsymbol{\nu} = [\nu_1 \ldots \nu_{N_T}]^T$. There are two sources of non-convexity in the problem in (10).[2] First, the functions $f_i(\boldsymbol{p}^J)$ and $g_i(\boldsymbol{p}^J)$ are both *posynomials*[3]; hence, each constraint in (10b) becomes the ratio of posynomials. Second, the objective function in (10a) is a posynomial, which should have been a *monomial* in a maximization problem [10, Sec. 4.5.2].

To obtain a convex approximation of (10), we define a collection of monomials as

$$\psi_{ijn}^{(\{\widetilde{\mathcal{A}}, \widetilde{\mathcal{J}}\})}(\boldsymbol{p}^J) \triangleq \lambda_{ij} \left(\frac{N_0}{2} \right)^n \prod_{k=1}^{N_{ij}-n} a_{\widetilde{\mathcal{A}}(k)}(\widetilde{\mathcal{J}}(k)) P_{\widetilde{\mathcal{J}}(k)}^J \tag{11}$$

where $N_{ij} \triangleq \left| \mathcal{A}_i^L \setminus \{j\} \right|$, $\mathcal{S}(k)$ denotes the kth element of a set $\mathcal{S}$ and $a_j(\ell)$ represents the ℓth element of $\boldsymbol{a}_j$. Then, using the arithmetic-geometric mean (AGM) inequality [11, Lemma 1], we can lower bound the posynomial $f_i(\boldsymbol{p}^J)$ by a monomial $\widetilde{f}_i(\boldsymbol{p}^J)$ so that $f_i(\boldsymbol{p}^J) \geq \widetilde{f}_i(\boldsymbol{p}^J)$, as shown in (12) on top of page 4, where $\mathcal{P}_k(\mathcal{S}) \triangleq \{\mathcal{B} \in \mathcal{P}(\mathcal{S}) : |\mathcal{B}| = k\}$ with $\mathcal{P}(\mathcal{S})$ denoting the power set of $\mathcal{S}$ and $\mathcal{M}_k(\mathcal{S}) \triangleq \{\mathcal{B} : |\mathcal{B}| = k \text{ and } \mathcal{B}(m) \in \mathcal{S}, m = 1, \ldots, k\}$. If the non-negative weights in (12) are chosen as

$$\mu_{ijn}^{(\{\widetilde{\mathcal{A}}, \widetilde{\mathcal{J}}\})} = \psi_{ijn}^{(\{\widetilde{\mathcal{A}}, \widetilde{\mathcal{J}}\})}(\boldsymbol{p}_\star^J)/f_i(\boldsymbol{p}_\star^J) \tag{13}$$

[1]It is assumed that λ_{ij}'s are strictly positive, i.e., $\xi_{ij} < 1$.

[2]Here, convexity refers to the condition that (10) can be represented in the form of a valid geometric program [10, Sec. 4.5.2].

[3]A *monomial* $f : \mathbb{R}_+^N \to \mathbb{R}$ is defined as $f(\boldsymbol{u}) = \vartheta \, u_1^{a_1} \, u_2^{a_2} \, \ldots \, u_N^{a_N}$ where $\vartheta \geq 0$ and $a_i \in \mathbb{R}$ for $i \in \{1, \ldots, N\}$, while a *posynomial* $f : \mathbb{R}_+^N \to \mathbb{R}$ is defined as the sum of monomials, i.e., $f(\boldsymbol{u}) = \sum_{m=1}^M \vartheta_m \, u_1^{a_{m,1}} \, u_2^{a_{m,2}} \, \ldots \, u_N^{a_{m,N}}$ [10].

for a power vector $\boldsymbol{p}^J_\star$, $\widetilde{f}_i(\boldsymbol{p}^J)$ becomes the best local monomial approximation to $f_i(\boldsymbol{p}^J)$ around $\boldsymbol{p}^J_\star$ according to the first order Taylor expansion and we have $f_i(\boldsymbol{p}^J_\star) = \widetilde{f}_i(\boldsymbol{p}^J_\star)$ [11]. Then, an approximated version of (10) is obtained as

$$\underset{\boldsymbol{p}^J,\boldsymbol{\nu}}{\text{maximize}} \;\; \boldsymbol{w}^T\boldsymbol{\nu} \tag{14a}$$

$$\text{subject to} \;\; \nu_i\, g_i(\boldsymbol{p}^J) \leq \widetilde{f}_i(\boldsymbol{p}^J),\; i=1,\ldots,N_T \tag{14b}$$

$$\text{(9b), (9c)}\;.$$

The problem in (14) is still non-convex due to the objective function in (14a). To convexify (14), we first express it in the epigraph form as follows:

$$\underset{\boldsymbol{p}^J,\boldsymbol{\nu},\eta}{\text{maximize}} \;\; \eta \tag{15a}$$

$$\text{subject to} \;\; \eta \leq \boldsymbol{w}^T\boldsymbol{\nu} \tag{15b}$$

$$\nu_i\, g_i(\boldsymbol{p}^J) \leq \widetilde{f}_i(\boldsymbol{p}^J),\; i=1,\ldots,N_T \tag{15c}$$

$$\text{(9b), (9c)}\;.$$

Then, using the AGM inequality for the posynomial $\chi(\boldsymbol{\nu}) \triangleq \boldsymbol{w}^T\boldsymbol{\nu}$ at the right-hand side (RHS) of (15b), we obtain its monomial approximation $\widetilde{\chi}(\boldsymbol{\nu})$ as

$$\chi(\boldsymbol{\nu}) = \boldsymbol{w}^T\boldsymbol{\nu} \geq \widetilde{\chi}(\boldsymbol{\nu}) \triangleq \prod_{i=1}^{N_T}\left(\frac{w_i\nu_i}{\kappa_i}\right)^{\kappa_i} \tag{16}$$

where the weights κ_i must be selected as

$$\kappa_i = (\nu_i^\star w_i)/\chi(\boldsymbol{\nu}^\star) \tag{17}$$

for a given $\boldsymbol{\nu}^\star$ to ensure that $\chi(\boldsymbol{\nu}^\star) = \widetilde{\chi}(\boldsymbol{\nu}^\star)$. Hence, replacing (15b) by its convex restricted version via (16), we obtain the following convex approximation of the original non-convex problem in (10):

$$\underset{\boldsymbol{p}^J,\boldsymbol{\nu},\eta}{\text{maximize}} \;\; \eta \tag{18a}$$

$$\text{subject to} \;\; \eta \leq \widetilde{\chi}(\boldsymbol{\nu}) \tag{18b}$$

$$\nu_i\, g_i(\boldsymbol{p}^J) \leq \widetilde{f}_i(\boldsymbol{p}^J),\; i=1,\ldots,N_T \tag{18c}$$

$$\text{(9b), (9c)}\;.$$

Now, the problem in (18) consists of a monomial objective and inequality constraints with posynomials and monomials on the left-hand side (LHS) and RHS, respectively. Therefore, (18) is a convex geometric program and can efficiently be solved by standard methods of convex optimization [10]. Overall, we can solve the original power allocation problem in (10) by solving a sequence of convex programs in the form of (18). Starting with an initial feasible vector $\left[\boldsymbol{p}_0^J\; \boldsymbol{\nu}_0\right]$, the problem in (18) can be solved using the monomial approximations $\widetilde{f}_i(\boldsymbol{p}^J)$ and $\widetilde{\chi}(\boldsymbol{\nu})$ around the current point at each iteration. This SCA procedure is summarized in Algorithm 1. In the following proposition, Algorithm 1 is shown to converge to a locally optimal Karush-Kuhn-Tucker (KKT) point of the original problem in (10).

Proposition 1. *Solving a series of convex geometric programs using the approximated problem* (18)*, Algorithm 1 converges to a locally optimal solution satisfying the KKT conditions of the original problem* (10) *(or, equivalently* (9)*).*

Proof: The proof can be constructed by following a similar approach to that in [11, Prop. 3]. ∎

B. Asymptotically Optimal Closed-Form Solution

In this part, we derive a closed-form power allocation solution to (9) that is asymptotically optimal as $P_{\mathrm{T}} \to 0$ and/or $\|\boldsymbol{a}_j\|_\infty \to 0$ for $j=1,\ldots,N_A$, where $\|\cdot\|_\infty$ is the l_∞ norm, as stated in Proposition 2, which can provide an important simplification to the jammer power allocation problem in (9) for small P_{T} and/or low channel gains between anchor and jammer nodes.[4]

Algorithm 1 GP-SCA Algorithm for Jammer Power Allocation

Initialization. Choose an initial feasible power vector $\boldsymbol{p}_0^J$ and auxiliary vector $\boldsymbol{\nu}_0$. Set $k=1$.
Iterative Step. At the kth iteration:
for $i=1,\ldots,N_T$ **do**
- Construct the monomial approximation $\widetilde{f}_i(\boldsymbol{p}^J)$ to the posynomial $f_i(\boldsymbol{p}^J)$ in (12) by computing the weights in (13) with $\boldsymbol{p}^J_\star = \boldsymbol{p}^J_{k-1}$.

end for
- Construct the monomial approximation $\widetilde{\chi}(\boldsymbol{\nu})$ to the posynomial $\chi(\boldsymbol{\nu})$ in (16) by setting $\boldsymbol{\nu}^\star = \boldsymbol{\nu}_{k-1}$ in (17).
- Solve the geometric program in (18) to obtain the optimal power vector $\boldsymbol{p}^J_{\mathrm{opt}}$ and the optimal auxiliary vector $\boldsymbol{\nu}_{\mathrm{opt}}$.
- Set $\boldsymbol{p}^J_k = \boldsymbol{p}^J_{\mathrm{opt}}$, $\boldsymbol{\nu}_k = \boldsymbol{\nu}_{\mathrm{opt}}$ and $k=k+1$.

Stopping Criterion. $|\eta_k - \eta_{k-1}| < \delta$ for some $\delta > 0$, where η_k denotes the optimal value of η in (18) at the kth iteration.

Proposition 2. Let $\boldsymbol{\zeta} \triangleq \sum_{i=1}^{N_T} w_i\,\bar{\boldsymbol{\lambda}}_i/\widetilde{\lambda}_i^2$, where $\bar{\boldsymbol{\lambda}}_i \triangleq \sum_{j_1\in\mathcal{A}_i^L}\sum_{\substack{j_2\in\mathcal{A}_i^L\\ j_2>j_1}}\sum_{j_3\in\mathcal{A}_i^L}\left[\lambda_{ij_1}\lambda_{ij_2}\lambda_{ij_3}\sin^2(\varphi_{ij_1}-\varphi_{ij_2})(\boldsymbol{a}_{j_1}+\boldsymbol{a}_{j_2}-\boldsymbol{a}_{j_3})\right]$ and $\widetilde{\lambda}_i \triangleq \sum_{j_1\in\mathcal{A}_i^L}\sum_{\substack{j_2\in\mathcal{A}_i^L\\ j_2>j_1}}\lambda_{ij_1}\lambda_{ij_2}\sin^2(\varphi_{ij_1}-\varphi_{ij_2})$ for $i\in\{1,\ldots,N_T\}$, $\boldsymbol{\theta}^J \triangleq \left[\boldsymbol{a}_1^T\boldsymbol{p}^J\ldots\boldsymbol{a}_{N_A}^T\boldsymbol{p}^J\right]^T$, $\widetilde{C}_i(\boldsymbol{\theta}^J) \triangleq C_i(\boldsymbol{p}^J)$, and $\widetilde{\boldsymbol{J}}_i(\boldsymbol{\theta}^J) \triangleq \boldsymbol{J}_i(\boldsymbol{p}^J)$. Assume that $\|\boldsymbol{a}_j\|_\infty \to 0$ for $j=1,\ldots,N_A$ and/or $P_T\to 0$. Then, the asymptotically optimal solution $\boldsymbol{p}^J_\star$ of (9) is given by

$$\boldsymbol{p}^J_\star(b_{\boldsymbol{\zeta}}(\ell)) = \min\left\{P_{\mathrm{T}} - \sum_{n=1}^{\ell-1}\boldsymbol{p}^J_\star(b_{\boldsymbol{\zeta}}(n)),\; P^{\mathrm{peak}}_{b_{\boldsymbol{\zeta}}(\ell)}\right\} \tag{19}$$

for $\ell\in\mathcal{J}$, where $b_{\boldsymbol{\zeta}}(\ell)$ denotes the index of the ℓth largest element of $\boldsymbol{\zeta}$ and $\boldsymbol{p}^J_\star(\ell)$ is the ℓth element of $\boldsymbol{p}^J_\star$.

Proof: As $\|\boldsymbol{a}_j\|_\infty \to 0$ for $j=1,\ldots,N_A$ and/or $P_T\to 0$, the objective function in (9) is approximated via the first order Taylor expansion around $\boldsymbol{\theta}^J = \boldsymbol{0}$ as

$$\sum_{i=1}^{N_T} w_i\widetilde{C}_i(\boldsymbol{\theta}^J) \approx \sum_{i=1}^{N_T} w_i\left(\widetilde{C}_i(\boldsymbol{0}) + \nabla\widetilde{C}_i(\boldsymbol{0})^T\boldsymbol{\theta}^J\right) \tag{20}$$

$$= \sum_{i=1}^{N_T} w_i\left(\widetilde{C}_i(\boldsymbol{0}) + \nabla\widetilde{C}_i(\boldsymbol{0})^T[\boldsymbol{a}_1\ldots\boldsymbol{a}_{N_A}]^T\boldsymbol{p}^J\right) \tag{21}$$

where $\widetilde{C}_i(\boldsymbol{\theta}^J) \triangleq C_i(\boldsymbol{p}^J)$ is used. After some manipulation, it can be calculated from (7) and (8) that $\nabla\widetilde{C}_i(\boldsymbol{0})^T[\boldsymbol{a}_1\ldots\boldsymbol{a}_{N_A}]^T = \bar{\boldsymbol{\lambda}}_i^T/\widetilde{\lambda}_i^2$. Hence, maximizing (21) for solving (9) is equivalent to

$$\underset{\boldsymbol{p}^J}{\text{maximize}} \;\; \boldsymbol{\zeta}^T\boldsymbol{p}^J \;\; \text{subject to} \;\; \text{(9b), (9c)}\,. \tag{22}$$

as $\|\boldsymbol{a}_j\|_\infty \to 0$ for $j=1,\ldots,N_A$ and/or $P_T\to 0$. As noted from (2), $\widetilde{\boldsymbol{J}}_i(\boldsymbol{\theta}^J)$ is monotonically decreasing in $\boldsymbol{\theta}^J$, i.e., $\widetilde{\boldsymbol{J}}_i(\boldsymbol{\theta}^J_1) \preceq \widetilde{\boldsymbol{J}}_i(\boldsymbol{\theta}^J_2)$ if $\boldsymbol{\theta}^J_1 \succeq \boldsymbol{\theta}^J_2$. Thus, $\widetilde{C}_i(\boldsymbol{\theta}^J)$ in (6) is a monotonically increasing function of $\boldsymbol{\theta}^J$, which makes $\nabla\widetilde{C}_i(\boldsymbol{0})$ and $\boldsymbol{\zeta}$ non-negative vectors. Therefore, similar to [3, Prop. 2], the optimal solution to (22) is derived as (19). ∎

[4] For example, when the jammer network has a sufficiently low power budget (e.g., to make jamming detection more difficult, or due to energy efficiency concerns) or when jammer nodes are distant from anchor nodes, one can employ the closed-form solution in Proposition 2 instead of Algorithm 1.

$$f_i(\boldsymbol{p}^J) = \sum_{j\in\mathcal{A}_i^L}\sum_{n=0}^{N_{ij}}\sum_{\substack{\widetilde{\mathcal{A}}\in\mathcal{P}_{N_{ij}-n}(\mathcal{A}_i^L\setminus\{j\})\\ \widetilde{\mathcal{J}}\in\mathcal{M}_{N_{ij}-n}(\mathcal{J})}} \psi_{ijn}^{(\{\widetilde{\mathcal{A}},\widetilde{\mathcal{J}}\})}(\boldsymbol{p}^J) \geq \widetilde{f}_i(\boldsymbol{p}^J) \triangleq \prod_{j\in\mathcal{A}_i^L}\prod_{n=0}^{N_{ij}}\prod_{\substack{\widetilde{\mathcal{A}}\in\mathcal{P}_{N_{ij}-n}(\mathcal{A}_i^L\setminus\{j\})\\ \widetilde{\mathcal{J}}\in\mathcal{M}_{N_{ij}-n}(\mathcal{J})}} \left(\frac{\psi_{ijn}^{(\{\widetilde{\mathcal{A}},\widetilde{\mathcal{J}}\})}(\boldsymbol{p}^J)}{\mu_{ijn}^{(\{\widetilde{\mathcal{A}},\widetilde{\mathcal{J}}\})}}\right)^{\mu_{ijn}^{(\{\widetilde{\mathcal{A}},\widetilde{\mathcal{J}}\})}} \quad (12)$$

IV. Numerical Results

Consider a wireless source localization system, where the anchor nodes are located at $[0\ 0]$, $[10\ 0]$, $[0\ 10]$ and $[10\ 10]$ m, target nodes reside at positions $\{[x\ y]\,|\,1 \leq x, y \leq 9 \text{ and } x, y \in \mathbb{Z}\}$ with equal probabilities (i.e., $1/81$), and the jammer nodes are located at $[1\ 4.5]$, $[9\ 5.5]$ and $[10\ 9.5]$ m. For this localization system, we evaluate the average CRLB performance in (9) achieved by Algorithm 1 (GP-SCA), the closed-form solution in Proposition 2 (see (19)), the uniform power allocation strategy, and the exhaustive search method (which solves (9) via exhaustive search). The uniform power allocation strategy assigns equal power levels to the jammer nodes; that is, $P_\ell^J = P_{\rm T}/N_J,\ \forall \ell \in \mathcal{J}$ for $P_{\rm T}/N_J \leq P_\ell^{\rm peak}$ [3]. In the simulations, N_0 is taken as 2 and the normalized version of the total power limit $P_{\rm T}$ is used as $\bar{P}_{\rm T} = 2P_{\rm T}/N_0$. Also, the peak power limits in (9c) are set to $P_\ell^{\rm peak} = 20,\ \forall \ell \in \mathcal{J}$. In addition, the free space path loss formulation with unit antenna gains and a carrier frequency of 23.87 MHz is considered, and $|\alpha_{ij}^1|^2$ in (3) and $|\gamma_{\ell j}|^2$ in (4) are modeled as $|\alpha_{ij}^1|^2 = \|\boldsymbol{x}_i - \boldsymbol{y}_j\|^{-2}$ and $|\gamma_{\ell j}|^2 = \|\boldsymbol{z}_\ell - \boldsymbol{y}_j\|^{-2}$, respectively [4]. Moreover, considering a zero path-overlap coefficient (i.e., $\xi_{ij} = 0$), λ_{ij} in (3) is expressed as $\lambda_{ij} = 4\pi^2 E_{ij}\beta_{ij}^2/(c^2\|\boldsymbol{x}_i - \boldsymbol{y}_j\|^2)$. Then, $E_{ij}\beta_{ij}^2 = \int f^2|S_{ij}(f)|^2 df = 4.56\times 10^{17}$ is used so that λ_{ij} is given by $\lambda_{ij} = 200\|\boldsymbol{x}_i - \boldsymbol{y}_j\|^{-2}$. (For example, $s_{ij}(t)$ with a rectangular spectrum of 500 kHz bandwidth around 23.87 MHz achieves this value for $E_{ij}/N_0 = 26$ dB.)

Fig. 1 illustrates the average CRLB in (9) corresponding to the different strategies against the normalized total power limit $\bar{P}_{\rm T}$. It is observed that the proposed algorithm in Algorithm 1 for solving the non-convex problem in (9) achieves the globally optimal solution found by the computationally expensive exhaustive search method for all power levels. This confirms the validity of Proposition 1 and further reveals that the proposed GP approach can indeed find global solutions without compromising the computational complexity[5]. In addition, the proposed power allocation method outperforms the uniform strategy and the performance gap becomes more significant as $\bar{P}_{\rm T}$ increases. Moreover, the closed-form solution derived in Proposition 2 achieves higher average CRLB than the uniform power allocation approach and performs similarly to Algorithm 1 for small values of $\bar{P}_{\rm T}$, in compliance with the asymptotic optimality property in Proposition 2. However, as $\bar{P}_{\rm T}$ increases, the closed-form solution deviates from the optimal one and even has lower performance than the uniform strategy after a certain level of $\bar{P}_{\rm T}$, as expected.

In Fig. 2, we show the average CRLBs obtained at each iteration of Algorithm 1 for various values of $\bar{P}_{\rm T}$. It is seen that Algorithm 1 converges to the global solution (identified by the exhaustive search technique) in approximately 15 iterations.

[5]With extensive simulations for various network configurations, it is seen that Algorithm 1 almost always attains the globally optimal solution of (9).

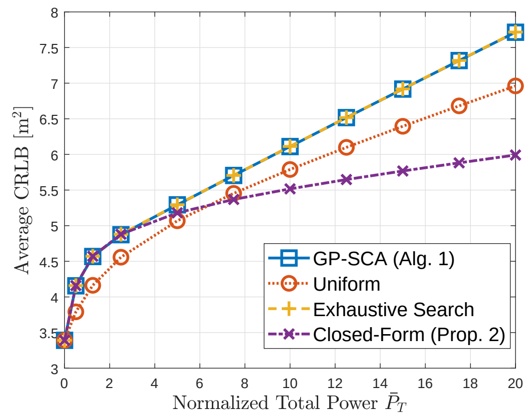

Fig. 1: Average CRLB for target nodes versus the normalized total power $\bar{P}_T$ for the considered power allocation strategies.

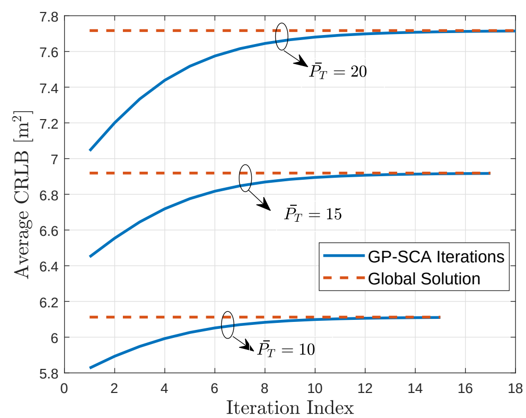

Fig. 2: Convergence behavior of Algorithm 1.

References

[1] R. Zekavat and R. M. Buehrer, *Handbook of Position Location: Theory, Practice and Advances*. John Wiley & Sons, 2011.

[2] M. Z. Win, et al. , "Network operation strategies for efficient localization and navigation," *Proc. IEEE*, vol. 106, no. 7, pp. 1224–1254, July 2018.

[3] S. Gezici, M. R. Gholami, S. Bayram, and M. Jansson, "Jamming of wireless localization systems," *IEEE Trans. Commun.*, vol. 64, no. 6, pp. 2660–2676, June 2016.

[4] S. Bayram, M. F. Keskin, S. Gezici, and O. Arikan, "Optimal power allocation for jammer nodes in wireless localization systems," *IEEE Trans. Signal Process.*, vol. 65, no. 24, pp. 6489–6504, Dec 2017.

[5] H. Hu and N. Wei, "A study of GPS jamming and anti-jamming," in *2nd Int. Conference on Power Electronics and Intelligent Transportation System (PEITS)*, vol. 1, Dec. 2009, pp. 388–391.

[6] Y. D. Zhang and M. G. Amin, "Anti-jamming GPS receiver with reduced phase distortions," *IEEE Signal Process. Lett.*, vol. 19, no. 10, pp. 635–638, Oct. 2012.

[7] M. Weiss and S. C. Schwartz, "On optimal minimax jamming and detection of radar signals," *IEEE Trans. Aerosp. Electron. Syst.*, vol. AES-21, no. 3, pp. 385–393, May 1985.

[8] Y. Shen and M. Z. Win, "Fundamental limits of wideband localization–part I: A general framework," *IEEE Trans. Inf. Theory*, vol. 56, no. 10, pp. 4956–4980, Oct. 2010.

[9] H. V. Poor, *An Introduction to Signal Detection and Estimation*. New York: Springer-Verlag, 1994.

[10] S. Boyd and L. Vandenberghe, *Convex Optimization*. Cambridge University Press, 2004.

[11] M. Chiang, et al., "Power control by geometric programming," *IEEE Trans. Wireless Commun.*, vol. 6, no. 7, pp. 2640–2651, July 2007.